Supplementary information

Tyrosine-based photoluminescent diketopiperazine supramolecular aggregates

Noritaka Shimosaraya,[a] Taichi Sotani,[a] Yu Miyagi,[a] Evan Angelo Quimada Mondarte,[b] Kasinan Suthiwanich,[b] Tomohiro Hayashi,[b] Yuuya Nagata,[c] Hiromitsu Sogawa[a] and Fumio Sanda*[a]

[a] Department of Chemistry and Materials Engineering, Faculty of Chemistry, Materials and Bioengineering, Kansai University
3-3-35 Yamate-cho, Suita, Osaka 564-8680, Japan

[b] Department of Materials Science and Engineering, School of Materials and Chemical Technology, Tokyo Institute of Technology
4259 Nagatsuta-cho, Midori-ku, Yokohama, Kanagawa 226-8503, Japan

[c] Institute for Chemical Reaction Design and Discovery, Hokkaido University
Kita 21, Nishi 10, Kita-ku, Sapporo, Hokkaido 001-0021, Japan

* Corresponding Author.

EXPERIMENTAL

Measurements

^{1}H (400 MHz) and ^{13}C NMR (100 MHz) spectra were recorded on JEOL JNM-ECS400 and JEOL JNM-ECA400 spectrometers. IR spectra were measured on a JASCO FT/IR-4100 spectrophotometer. ESI-TOF-MS measurement was performed on a Shimadzu LCMS-IT-TOF mass spectrometer. Melting points (mp) were measured on a Yanaco micro melting point apparatus. Number-average molecular weight (M_n) and polydispersity ($Đ$) values of a polymer were determined by size exclusion chromatography (SEC) on a JASCO HPLC system consisting of PU-4580, DG-980-50, CO-965, UV-4570 and RI-930, equipped with TOSOH TSK-GEL α-M and GMH$_{XL}$ columns, using a solution of LiBr (10 mM) in *N,N*-dimethylformamide (DMF) as an eluent at a flow rate of 1.0 mL/min, calibrated by polystyrene standards at 40 °C. UV-vis absorption spectra were measured in a quartz cell (optical distance: 1 cm) using a JASCO V-550 spectrophotometer. Photoluminescence spectra were measured in a quartz cell (optical distance: 1 cm) using a JASCO FP-750 fluorescence spectrophotometer. The absolute photoluminescence quantum yields were measured in a quartz cell (optical distance: 1 cm) using a HITACHI F-7000 fluorescence spectrophotometer equipped with an integration sphere. CD and UV–vis absorption spectra were measured in a quartz cell (optical path length: 1 cm) using a JASCO J-820 spectropolarimeter. DLS was measured in a square glass cell using a Malvern Instruments Zetasizer Nano ZSP spectrophotometer. Transmission electron microscope (TEM) observation was performed on a JEOL JEM-1210 electron microscope. Atomic force microscope (AFM) images were obtained using a commercial AFM system (MPF-3D, Oxford Instruments, UK). For the preparation of the sample for AFM, a silicon substrate was first cleaned by ultrasonication in acetone, then in ethanol, and finally in pure water (18.2 MΩ) (15 minutes in each solvent), followed by drying under nitrogen flow. Then, a drop of a solution of **1** in DMSO (0.2 w/v%) was placed on the silicon substrate and dried under ambient conditions. The image in Fig. 6 was obtained by fast force mapping using a sharp tetrahedral tip (tip radius < 10 nm, nominal spring constant = 0.2 N/m, ATEC-CONT, Nanosensors) at a scan size of 500 nm^2 with 256 × 256 scan points. The other AFM images found in Fig. S7.1-10.2 were obtained in the amplitude-modulation mode and fast force mapping using different types of probes. More details on the measurements for the supporting figures can be found in their captions. Fluorescence microscopic observation was performed on an OLYMPUS fluorescence microscope IX71.

Materials

All reagents were commercially obtained and used without further purification unless otherwise stated. DMF was purified by distillation over CaH_2. Di-*tert*-butyl dicarbonate (Boc_2O) was offered by Tokuyama corporation. Silica gel 60 (Wako, Wakogel 60N, 63–212 μm mesh) was used for column chromatography. Phenyl *N*-phenylcarbamate (**2**) was synthesized by the reaction of aniline and phenyl isocyanate, and the structure was confirmed by comparison of spectroscopic data with those in the literature.[S1,S2] Tetrahydrofuran (THF) containing no stabilizer was treated by nitrogen bubbling to remove oxygen, and used for photoluminescence measurements.

Syntheses

L-Tyrosine Methyl Ester. L-Tyrosine (20.05g, 120.0 mmol) and MeOH (200 mL) were fed into a reaction vessel, and the resulting mixture was stirred at room temperature for 30 minutes. Thionyl chloride (16 mL, 220 mmol) was added to the mixture dropwise using a dropping funnel, and the mixture was stirred at room temperature overnight. The solvent was removed using a rotary evaporator, and the residue was dried under reduced pressure to obtain a white solid. It was dissolved in ethyl acetate (200 mL), and the solution was subsequently washed with pure water and

0.5 M NaOH aqueous solution. The organic layer was separated from the aqueous layer, dried over anhydrous $MgSO_4$, concentrated on a rotary evaporator, and dried under reduced pressure to obtain L-tyrosine methyl ester (20.1 g, 35.9 mmol) as a white solid in 72% yield. ^1H NMR (400 MHz, DMSO-d_6): δ 1.66 (s, 2H, $-NH_2$), 2.59–2.71 (m, 2H, $-CH_2-$), 3.43 (t, $J = 6.8$ Hz, 1H, chiral –CH<), 3.51 (s, 3H, $-OCH_3$), 6.60–6.9x (m, 4H, Ar), 9.20 (s, 1H, –OH).

L-Tyrosine DKP. L-Tyrosine methyl ester (5 g, 25.6 mmol), toluene (13 mL) and EtOH (13 mL) were fed into a reaction vessel, and the resulting mixture was stirred at 100 °C for 5 days. The mixture was concentrated on a rotary evaporator to obtain a solid. It was separated by filtration and washed with $CHCl_3$ to obtain L-tyrosine DKP (2.39 g, 7.32 mmol) as a white solid in 29% yield; mp 264–266 °C (decomposition). ^1H NMR (400 MHz, DMSO-d_6): δ 2.05–2.06 (m, 4H, $-CH_2-$), 3.81 (s, 2H, chiral >CH–), 6.63–7.00 (m, 8H, Ar), 7.76 (s, 2H, –NH–), 9.2 (s, 2H, –OH). ^{13}C NMR (100 MHz, DMSO-d_6): δ 56.25 (stereogenic C), 115.56 (Ar), 127.04 (Ar), 131.29 (Ar) 156.60 (Ar), 166.79 (–CONH–). IR (cm^{-1}, KBr): 3204, 2960, 2918, 1670 (–NHCO–), 1516, 1458, 1243. ESI-TOF-MS (negative) Calcd. for $C_{18}H_{18}N_2O_4$: 326.1267. Found: 326.1225.

Compound 1. L-Tyrosine DKP (1.0 g, 3.0 mmol) and phenyl isocyanate (144 mg, 0.3 mmol) were fed into a reaction vessel under Ar. $Bu_2Sn(OCOC_{11}H_{23})_2$ (0.09 mL, 0.15 mmol) and DMF (6 mL) were fed into the vessel, and the resulting mixture was stirred at 50 °C for 24 hours. The reaction mixture was poured into Et_2O (40 mL) and the precipitated solid was separated by filtration. The obtained solid was dissolved in DMF; a large volume of hexane was added to the mixture, and the precipitated solid was separated by filtration to obtain **1** in 96% yield; mp 245–250 °C (decomposition). ^{1}H NMR (400 MHz, DMSO-d_6): δ 2.57–2.62 (dd, J = 13.6 Hz, 4.4 Hz, 2H, –CH_2–), 2.87–2.91 (dd, J = 9.6, 3.2 Hz, 2H, –CH_2–), 3.85 (s, 2H, >CH–), 6.55–7.20 (m, 18H, Ar), 7.93 (s, 2H, DKP –NH–), 9.29 (s, 2H, urethane –NH–). ^{13}C NMR (100 MHz, DMSO-d_6): δ 55.34 (–CH_2–), 56.26 (>CH–), 114.37, 115.32, 115.56, 116.12, 126.31, 127.03, 129.32, 131.28, 131.60 (Ar) 156.62 (C–OH), 166.80 (DKP, –CONH–), 167.58 (urethane, –CONH–). IR (cm^{-1}, KBr): 3238, 1670, 1516, 1238, 826, 754. ESI-TOF-MS (positive) Calcd. for $C_{32}H_{28}N_4O_6$: 564.2009. Found: 564.1986.

Polymer 2*p*. Compound **1** (100 mg, 0.3 mmol) and 1,4-phenylene diisocyanate (48 mg, 0.3 mmol) were fed into a reaction vessel purged with Ar. $Bu_2Sn(OCOC_{11}H_{23})_2$ (0.01 mL, 0.015 mmol) and

DMF (6 mL) were fed into the vessel, and the resulting mixture was stirred at 50 °C for 20 h. The polymerization mixture was poured into Et_2O (40 mL), and the precipitated solid was separated by filtration to obtain a polymer in 96% yield. ^{1}H NMR (400 MHz, DMSO-d_6): δ 6.56–6.89 (4H, –$(CH_2)_2$–), 7.30–7.34 (8H, –$(CH_2)_2$–), 7.77 (2H, –NHCO–), 9.23 (2H, –NHCO–). IR (cm^{-1}, KBr): 3306, 2959, 2920, 1670 (–NHCO–), 1513. M_n 1,200, *Đ* 1.7.

Computation

All calculations were carried out on the supercomputer systems, Academic Center for Computing and Media Studies, Kyoto University, and Information Initiative Center, Hokkaido University. Semiempirical and DFT calculations were performed with the GAUSSIAN 16 program,[S3] Rev B.01 and C.01, using the PM7,[S4] B3LYP-D3[S5,S6] and M06-2X[S7,S8] functionals in conjunction with the 6-31G* basis set. The reduced density gradient isosurface representing the intermolecular interactions was visualized using NCIPLOT.[S9] MD simulations were performed with AMBER 16 using the ff14SB force field.[S10] A tetrahydrofuran (THF) box for MD simulations was constructed using PACKMOL.[S11]

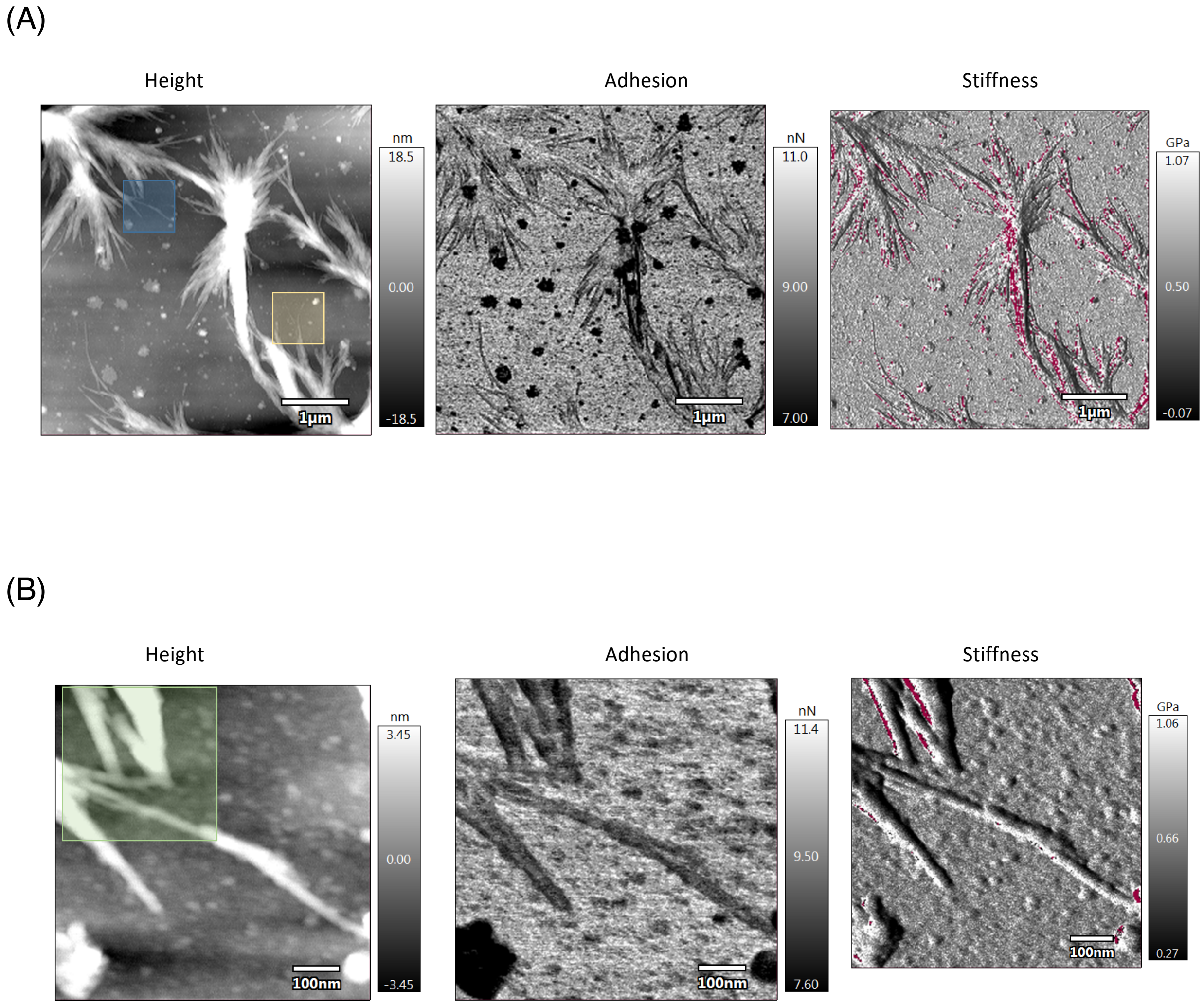

Fig. S1.1 AFM images of **1**. Zoom region 1. Force mapping by ATEC-cont. k = 0.3 N/m, resonance freq = 15 kHz, tip radius < 10 nm. Z-rate: 100 Hz, points & lines: 256×256 set point: 5.24 nN. (A) Blue box = zoomed region 1 [Fig. S1.1, (B) and Fig. S1.2 (C)], yellow box = zoomed region 2 [Fig. S1.2, (D)]. (B) Zoom region 1. Green box = zoomed region shown on Fig. S1.2, (C).

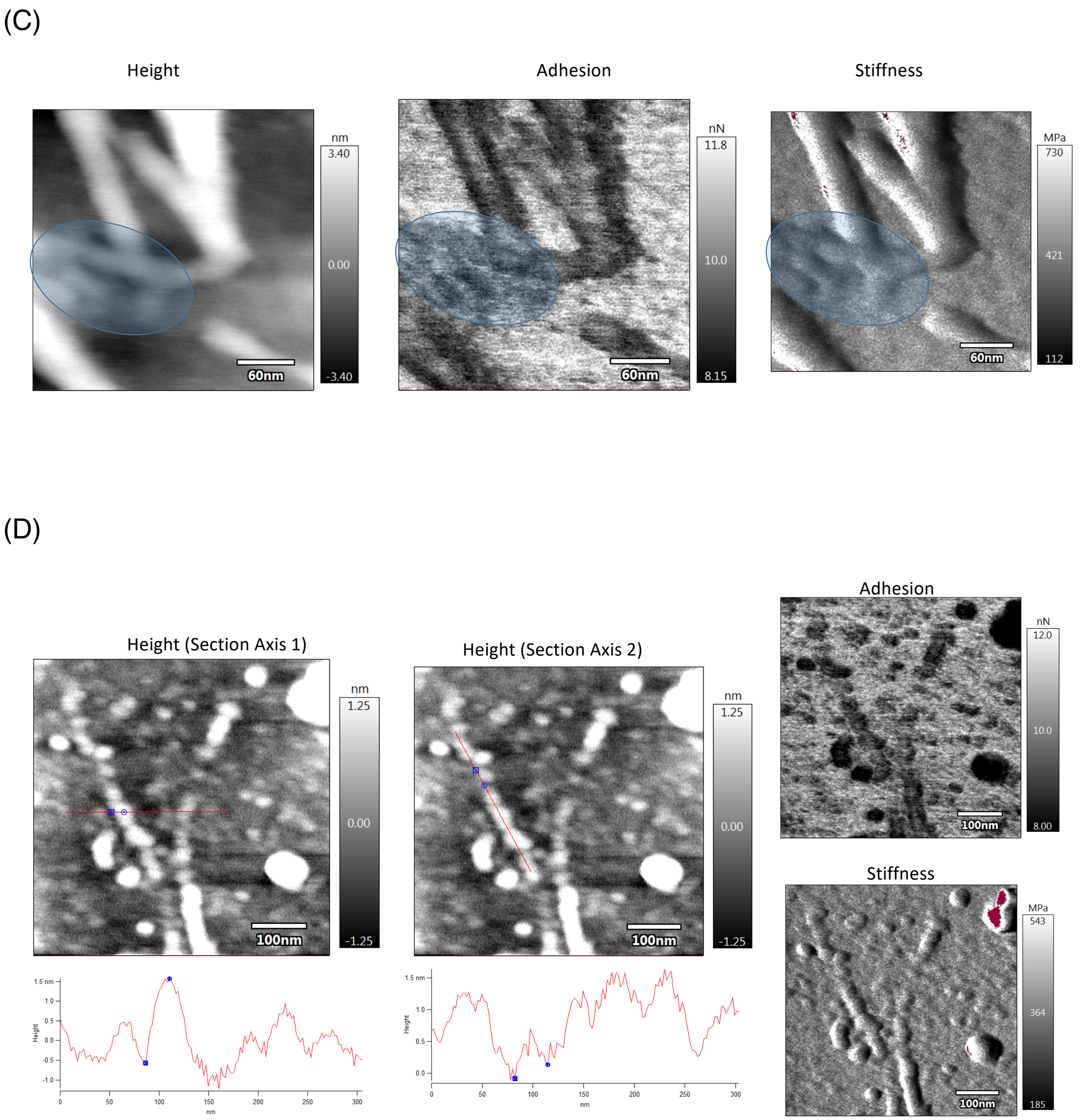

Fig. S1.2 AFM images of **1**. Force mapping by ATEC-cont. k = 0.3 N/m, resonance freq = 15 kHz, tip radius < 10 nm. Z-rate: 100 Hz, points & lines: 256×256 set point: 5.24 nN. (C) Zoom region 1. Blue oval = hint of a helical shape. (D) Zoomed region 2.

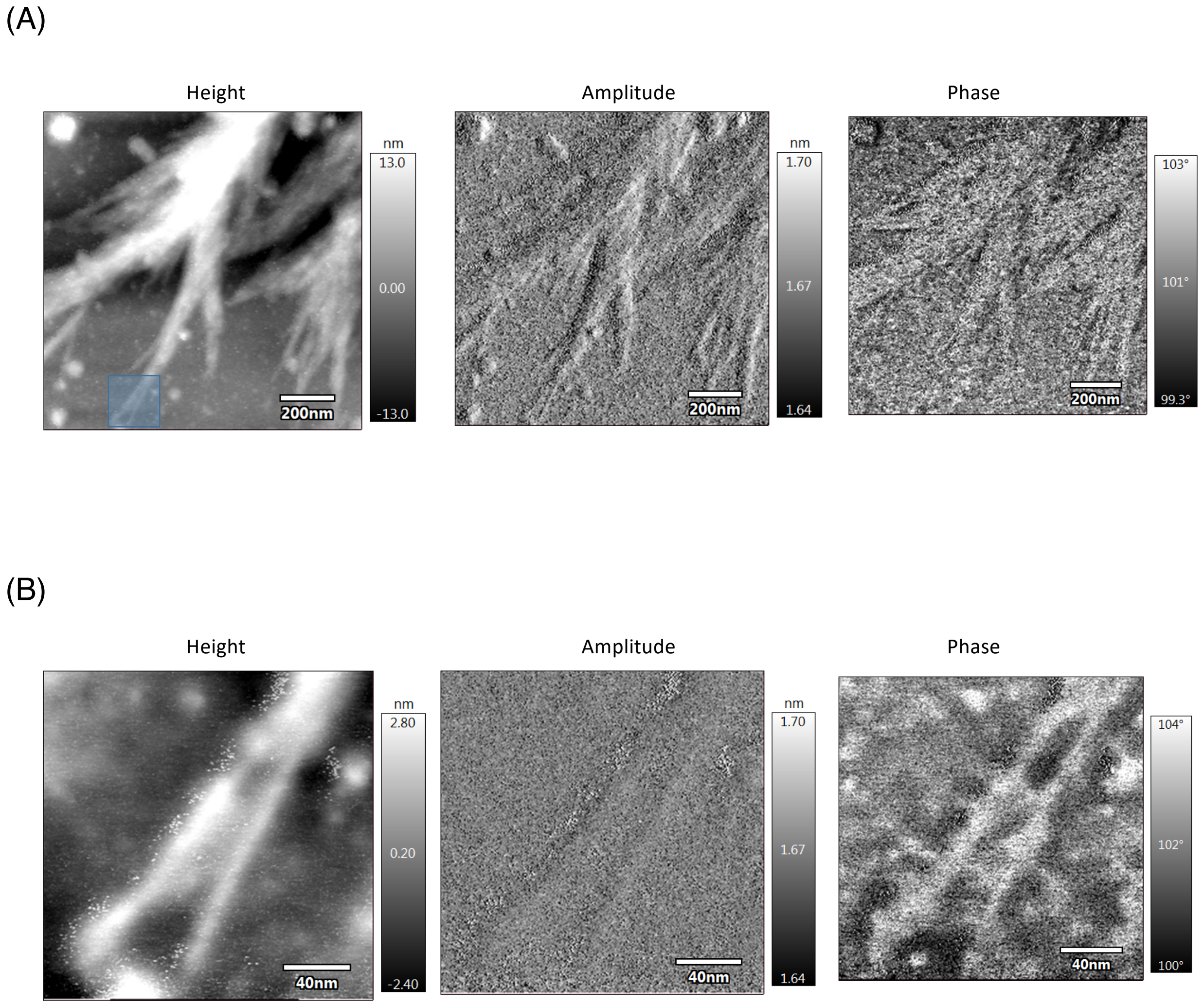

Fig. S2 AFM images of **1**. Position 1. AC imaging by super-sharp Si tip. k = 21.3 N/m. Resonance freq = 330 kHz, tip radius: 2–5 nm. Scan rate: 0.3 Hz, points & lines: 256×256, free air amp: 2.05 nm, set point amp: 1.66 nm. (A) blue box = zoomed region shown in Fig. S2, (B). (B) Zoomed region of position 1.

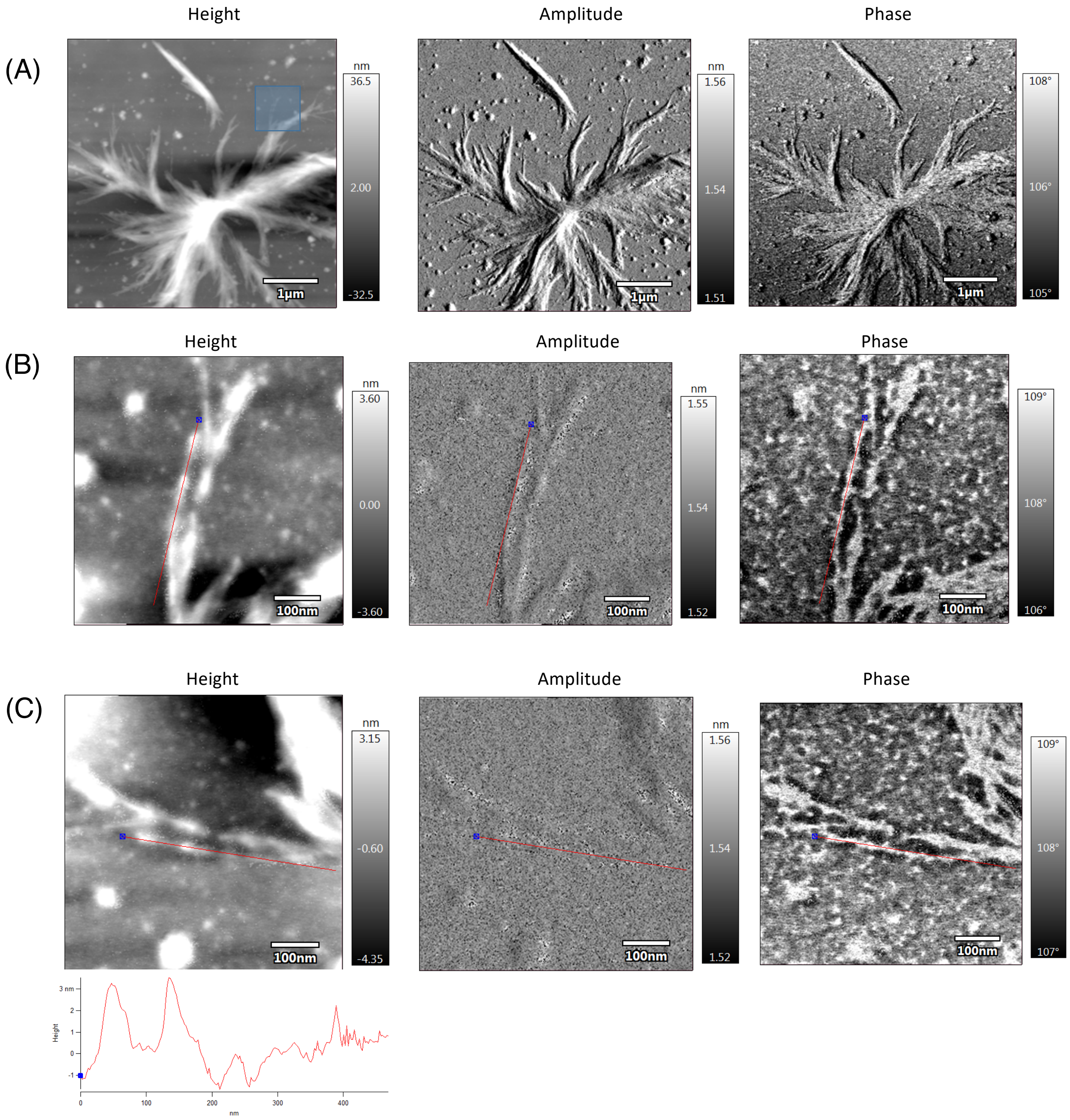

Fig. S3 AFM images of **1**. Position 2. AC imaging by super-sharp Si tip. k = 21.3 N/m. Resonance freq = 330 kHz, tip radius: 2–5 nm. Scan rate: 0.1 Hz, points & lines: 256×256, free air amp: 1.82 nm, set point amp: 1.53 nm. (A) blue box = zoomed region shown in Fig. S3, (B) and (C). (B) Zoomed region. (C) Zoomed region. Scan angle: 90°

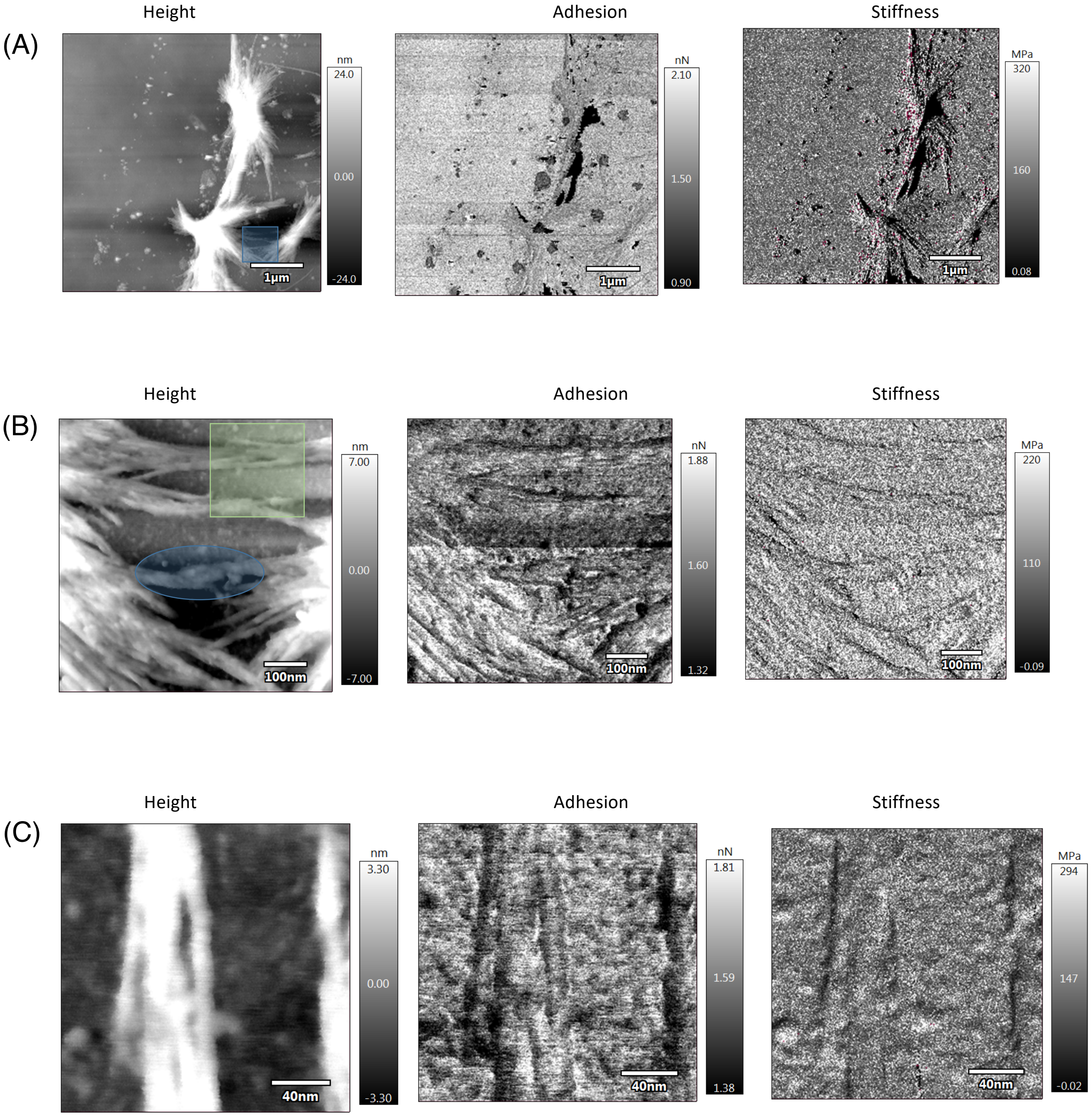

Fig. S4.1 AFM images of **1**. Force mapping by biolever mini. k = 0.1 N/m, resonance freq = 100 kHz, tip radius = 8 nm. Z-rate: 200Hz, points & lines: 256×256, set point: 200 pN. (A) Blue box = zoomed region shown in Fig. S4.1, (B). (B) Green box = zoomed region shown in Fig. S4.1, (C). Blue oval = interesting bigger helical bundle of fibers. (C) Scan angle: 90°.

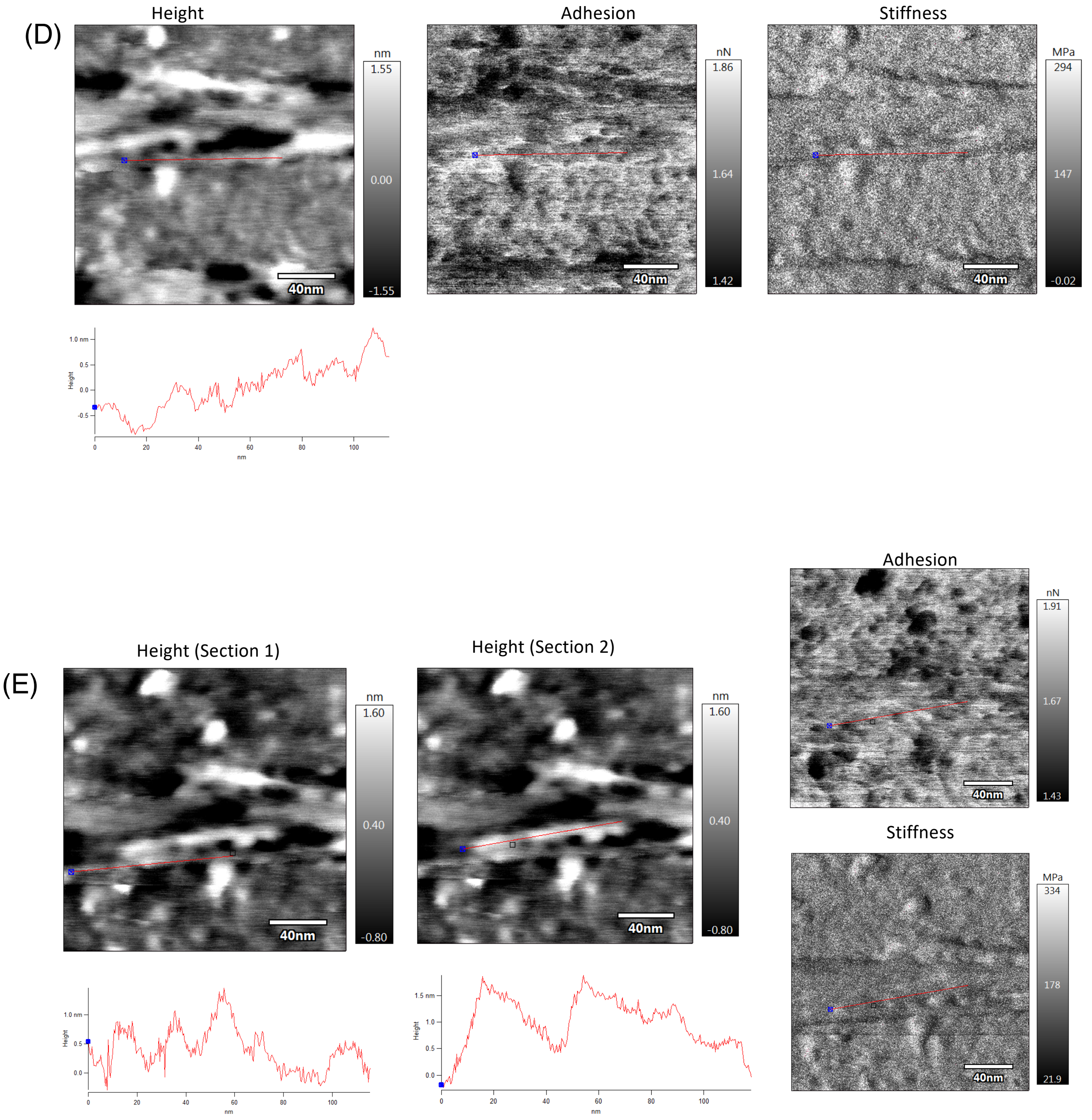

Fig. S4.2 AFM images of **1**. Force mapping by biolever mini. k = 0.1 N/m, resonance freq = 100 kHz, tip radius = 8 nm. Z-rate: 200Hz, points & lines: 256×256, set point: 200 pN. (D) Scan angle: 0°. (E) Scan angle: 0°. Points & lines: 512×512.

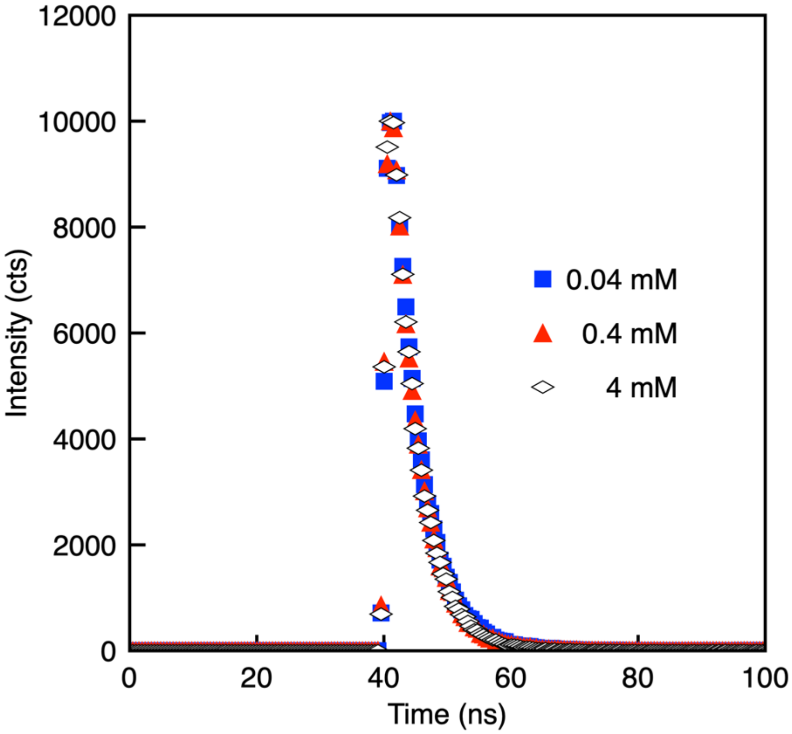

Fig. S5 Photoluminescence decay curves of **1** excited at 280 nm measured in THF (*c* = 0.04, 0.4 and 4 mM) at 25 °C. The photoluminescence lifetimes were 4.2, 4.1 and 4.0 ns at *c* = 0.04, 0.4 and 4 mM, respectively.

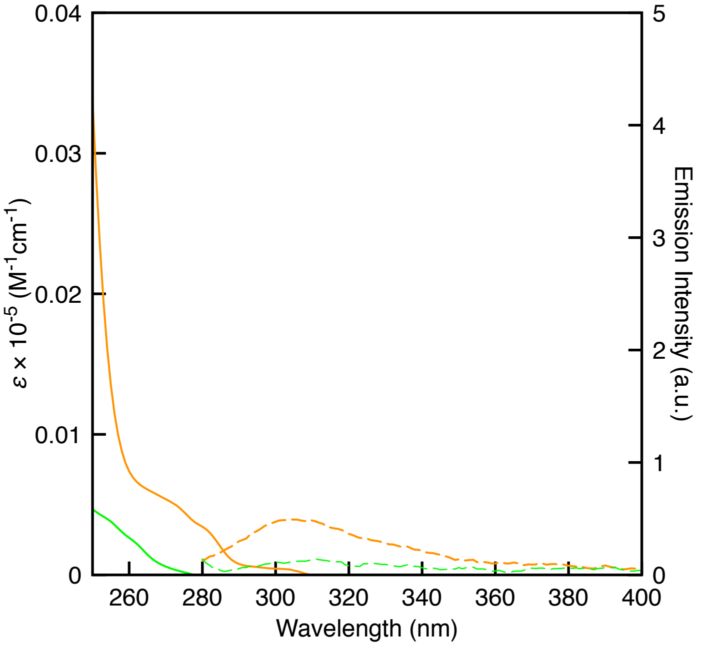

Fig. S6 Absorption (solid lines) and emission (dashed lines, excited at 280 nm) spectra of benzene (green) and **2** (orange) measured in THF (c = 0.04 mM) at 25 °C.

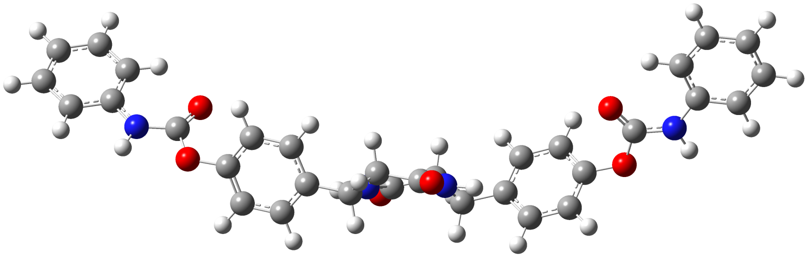

Excited State 1: Singlet-A, 4.8649 eV, 254.86 nm, *f* = 0.0650, <S**2> = 0.000

#144 — #149 0.12690

#144 — #157 0.17777

#148 — #153 -0.61981

#148 — #154 0.14921

This state for optimization and/or second-order correction.

Total Energy, E(TD-HF/TD-DFT) = -1905.84341320 au.

Copying the excited state density for this state as the 1-particle RhoCI density.

Fig. S7 Conformer of **1** optimized by the TD-DFT method [M06-2X/6-31+G*, nstates = 3, root = 1, SCRF (solvent = THF)].

#157 (LUMO + 8)

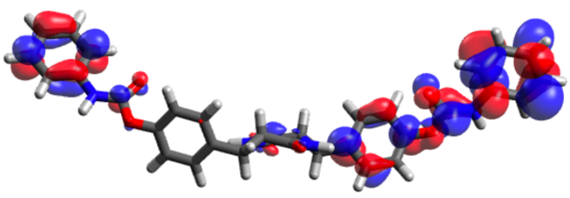

#153 (LUMO + 4)

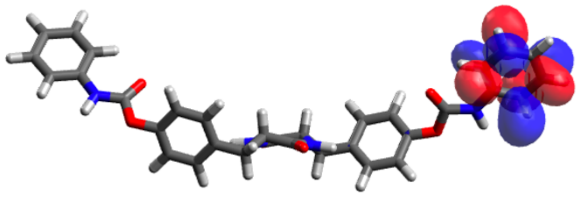

#156 (LUMO + 7)

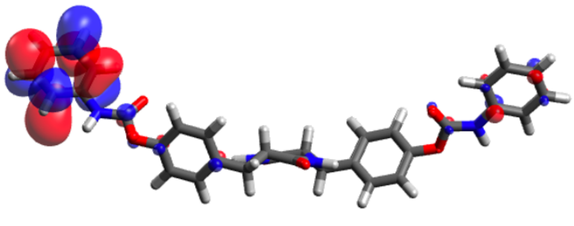

#152 (LUMO + 3)

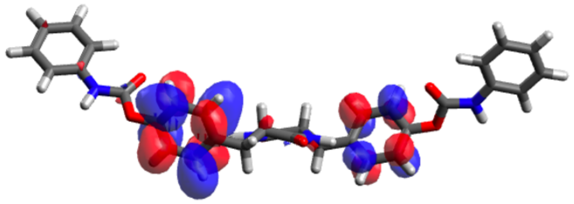

#155 (LUMO + 6)

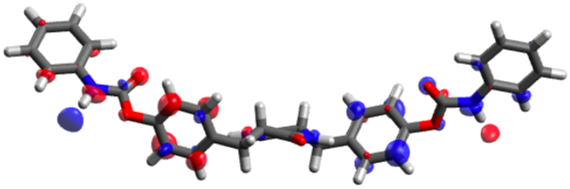

#151 (LUMO + 2)

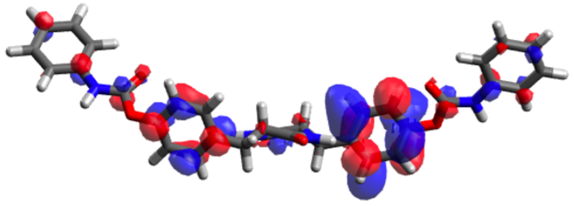

#154 (LUMO + 5)

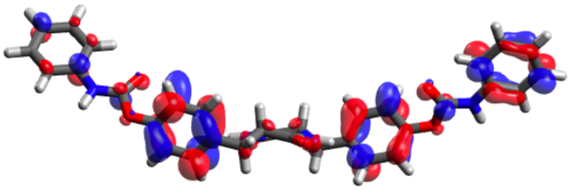

#150 (LUMO + 1)

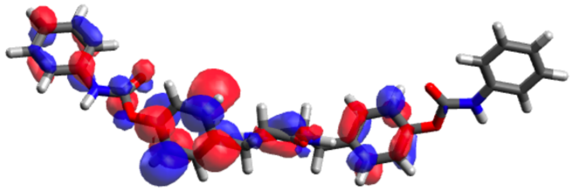

Fig. S8.1 Shapes of representative MOs of unimolecular model of **1**, including the MOs contributing to the excited state 1 depicted in Fig. S7. The geometries were optimized by the TD-DFT method [M06-2X/6-31+G*, nstates = 3, root = 1, SCRF (solvent = THF)].

#149 (LUMO)

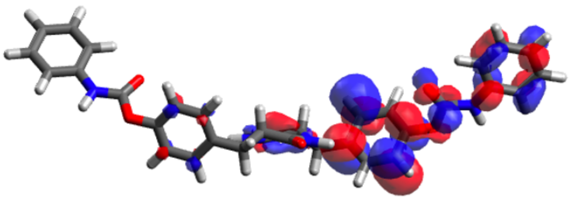

#148 (HOMO)

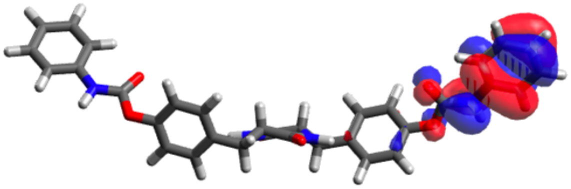

#147 (HOMO – 1)

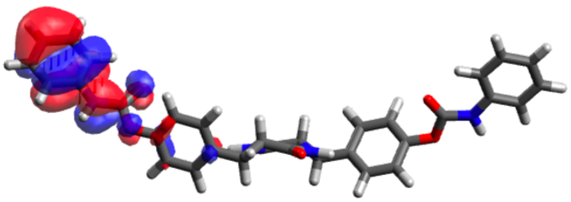

#146 (HOMO – 2)

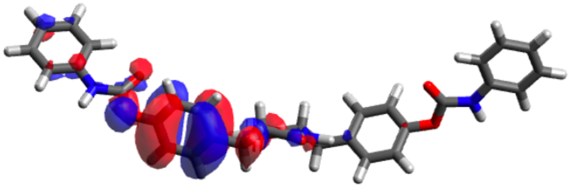

#145 (HOMO – 3)

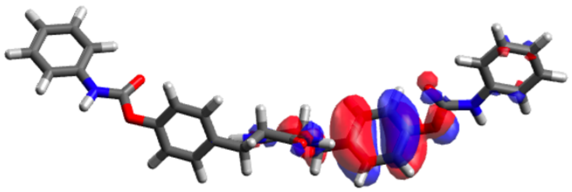

#144 (HOMO – 2)

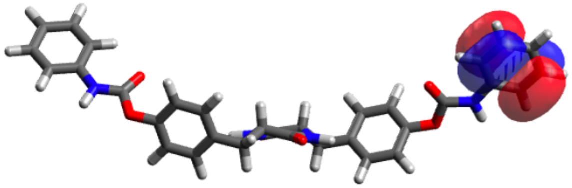

Fig. S8.2 Shapes of representative MOs of unimolecular model of **1**, including the MOs contributing to the excited state 1 depicted in Fig. S7. The geometries were optimized by the TD-DFT method [M06-2X/6-31+G*, nstates = 3, root = 1, SCRF (solvent = THF)].

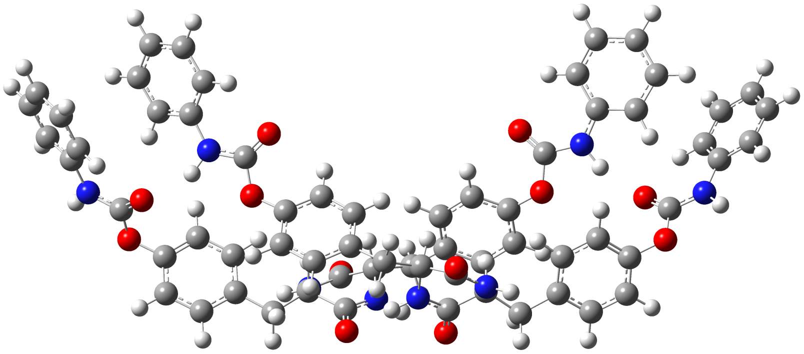

Excited State 1: Singlet-A, 4.6477 eV, 266.77 nm, *f* = 0.1140, <S**2> = 0.000

#290 — #298 -0.10690
#296 — #297 -0.18849
#296 — #298 0.37715
#296 — #299 0.14185
#296 — #300 0.24896
#296 — #303 0.18904
#296 — #304 -0.11462
#296 — #313 -0.14543
#296 — #314 0.18526
#296 — #315 -0.15232
#296 — #318 0.10056

This state for optimization and/or second-order correction.
Total Energy, E(TD-HF/TD-DFT) = -3811.90645004 au.
Copying the excited state density for this state as the 1-particle RhoCI density.

Fig. S9 Conformer of a dimer model of **1** optimized by the TD-DFT method [M06-2X/6-31+G*, nstates = 3, root = 1, SCRF (solvent = THF)].

#318 (LUMO + 21)

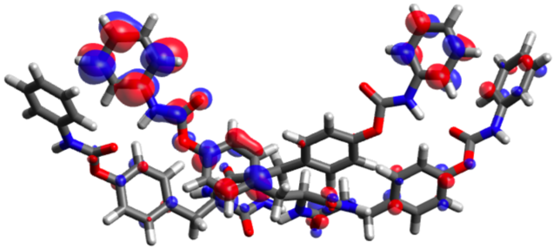

#317 (LUMO + 20)

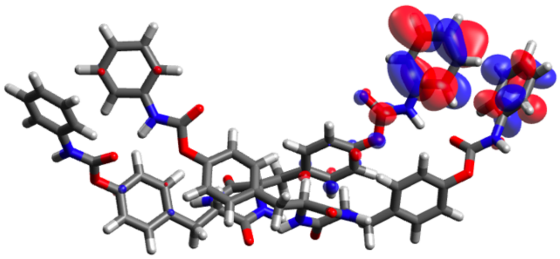

#316 (LUMO + 19)

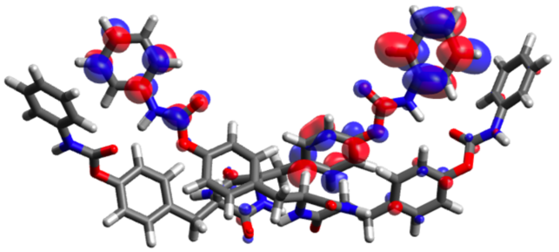

#315 (LUMO + 18)

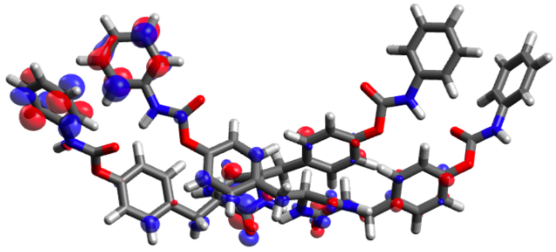

#314 (LUMO + 17)

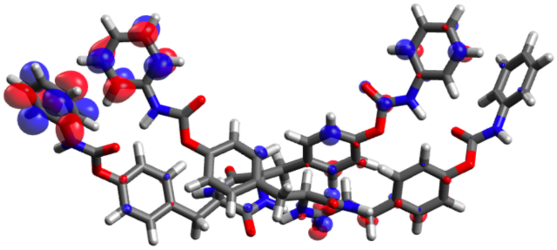

#313 (LUMO + 16)

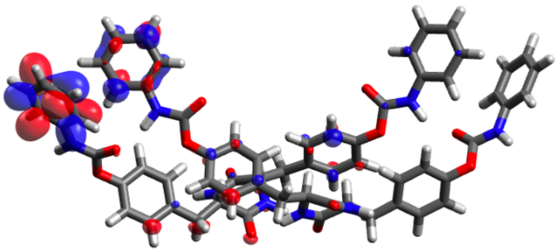

Fig. S10.1 Shapes of representative MOs of dimolecular model of **1**, including the MOs contributing to the excited state 1 depicted in Fig. S9. The geometries were optimized by the TD-DFT method [M06-2X/6-31+G*, nstates = 3, root = 1, SCRF (solvent = THF)].

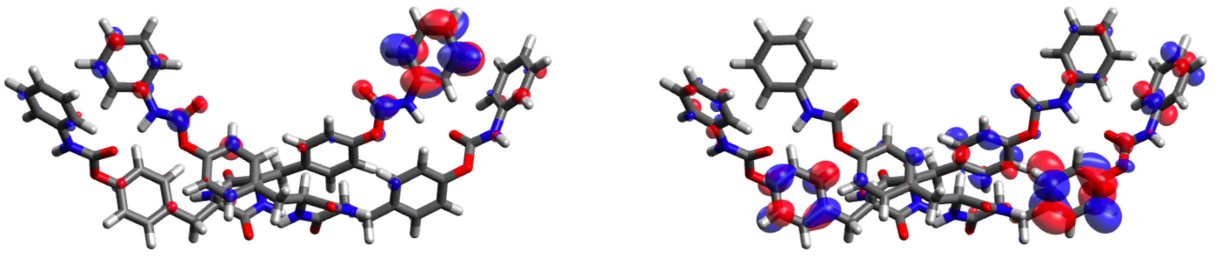

#312 (LUMO + 15)

#309 (LUMO + 12)

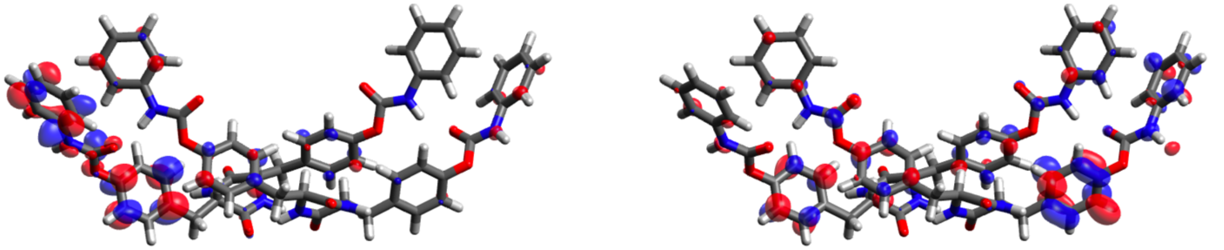

#311 (LUMO + 14)

#308 (LUMO + 11)

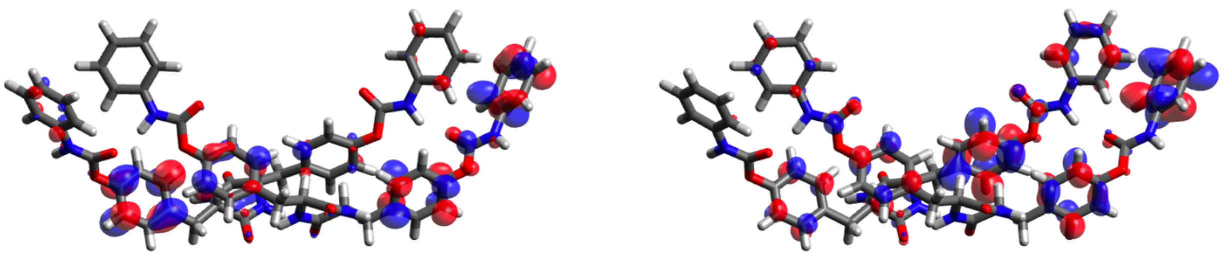

#310 (LUMO + 13)

#307 (LUMO + 10)

Fig. S10.2 Shapes of representative MOs of dimolecular model of **1**, including the MOs contributing to the excited state 1 depicted in Fig. S9. The geometries were optimized by the TD-DFT method [M06-2X/6-31+G*, nstates = 3, root = 1, SCRF (solvent = THF)].

#306 (LUMO + 9)

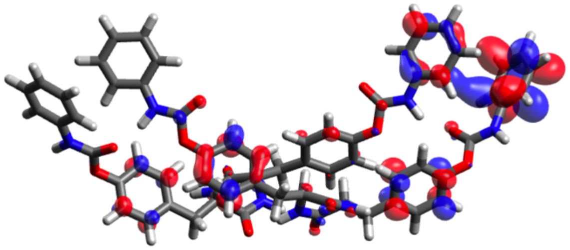

#303 (LUMO + 6)

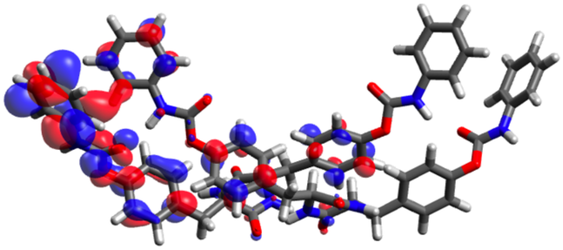

#305 (LUMO + 8)

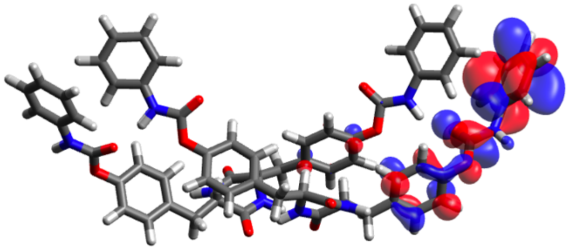

#302 (LUMO + 5)

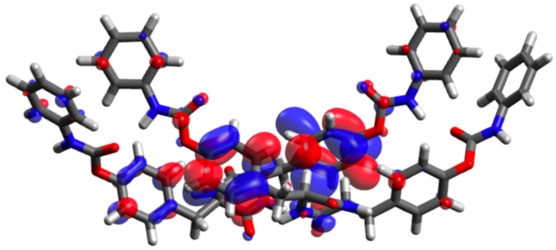

#304 (LUMO + 7)

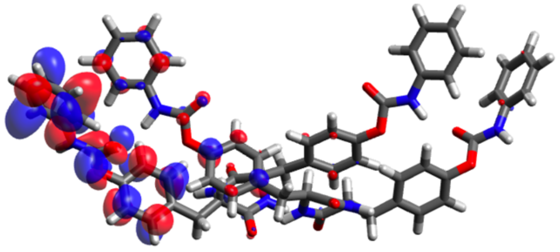

#301 (LUMO + 4)

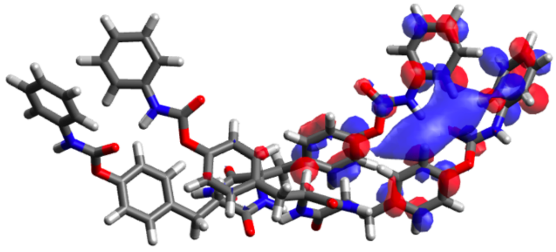

Fig. S10.3 Shapes of representative MOs of dimolecular model of **1**, including the MOs contributing to the excited state 1 depicted in Fig. S9. The geometries were optimized by the TD-DFT method [M06-2X/6-31+G*, nstates = 3, root = 1, SCRF (solvent = THF)].

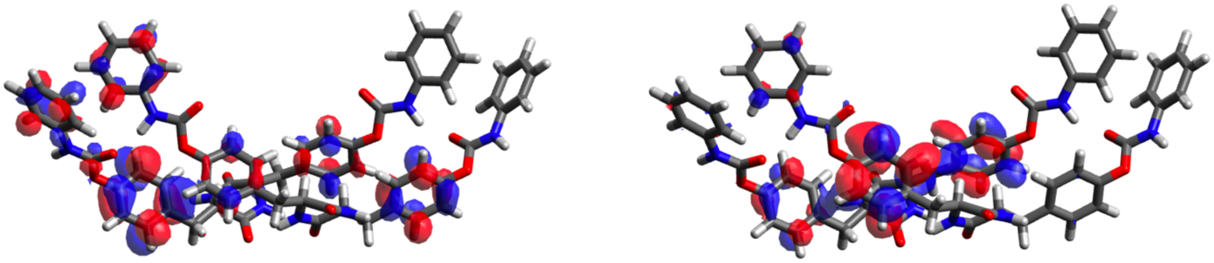

#300 (LUMO + 3)

#297 (LUMO)

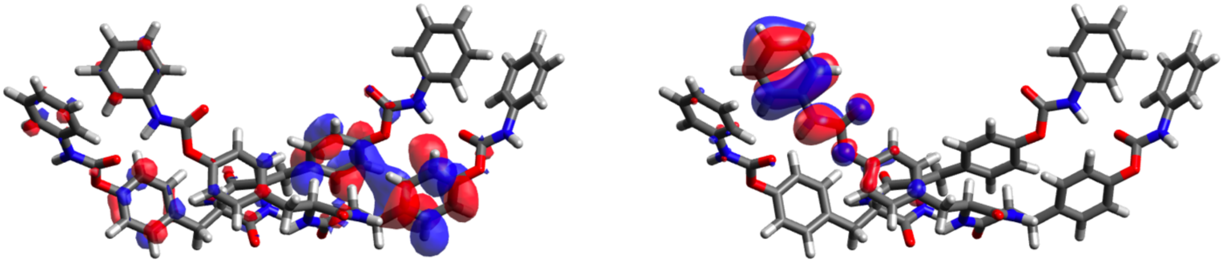

#299 (LUMO + 2)

#296 (HOMO)

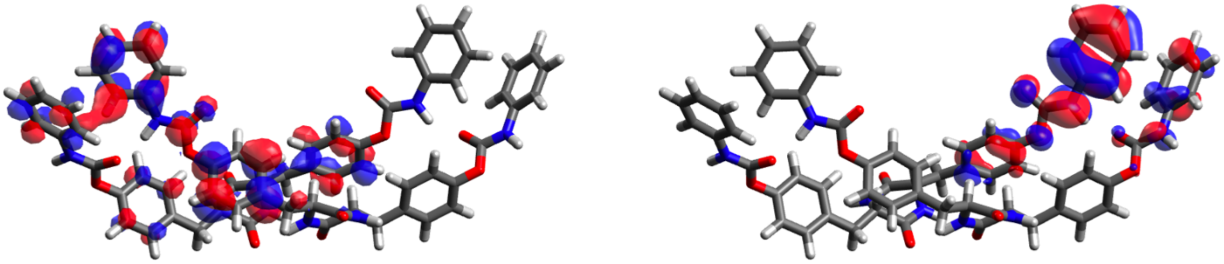

#298 (LUMO + 1)

#295 (HOMO – 1)

Fig. S10.4 Shapes of representative MOs of dimolecular model of **1**, including the MOs contributing to the excited state 1 depicted in Fig. S9. The geometries were optimized by the TD-DFT method [M06-2X/6-31+G*, nstates = 3, root = 1, SCRF (solvent = THF)].

#294 (HOMO – 2)

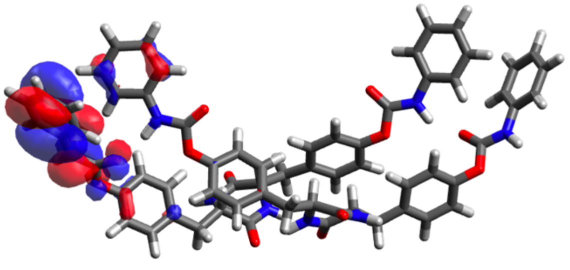

#293 (HOMO – 3)

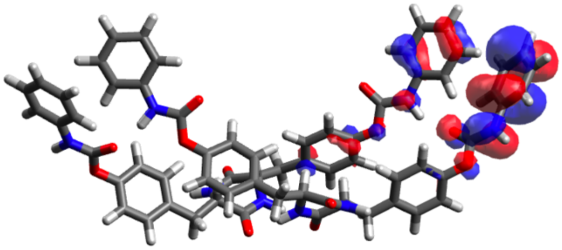

#292 (HOMO – 4)

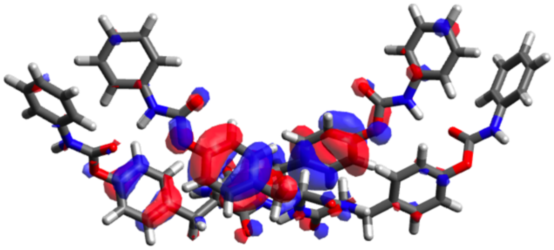

#291 (HOMO – 5)

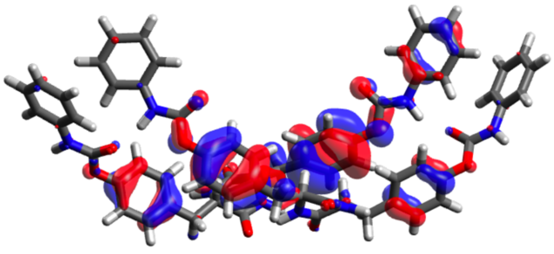

#290 (HOMO – 6)

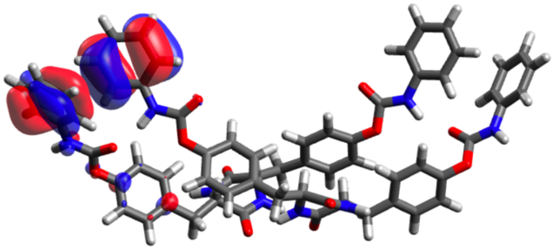

Fig. S10.5 Shapes of representative MOs of dimolecular model of **1**, including the MOs contributing to the excited state 1 depicted in Fig. S9. The geometries were optimized by the TD-DFT method [M06-2X/6-31+G*, nstates = 3, root = 1, SCRF (solvent = THF)].

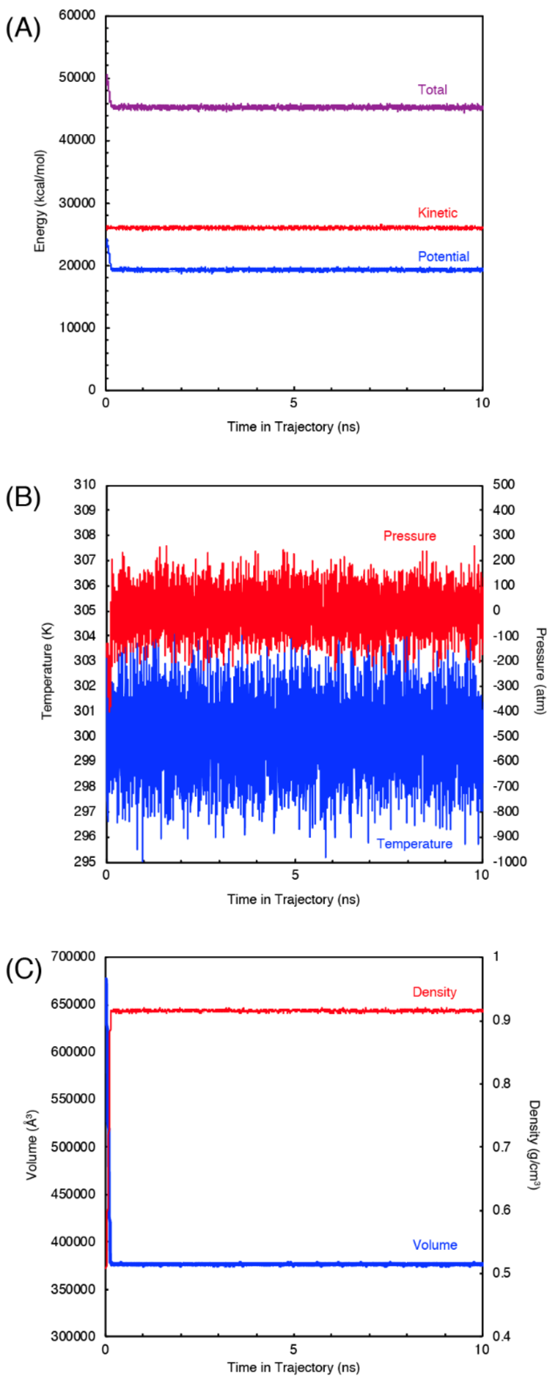

Fig. S11 (A) total and potential energies, (B) temperature and pressure, (C) volume and density obtained by the MD simulation of a 32-mer of **1** in a solvent box consisting of 2,662 THF molecules at 300 K for 0–10 ns.

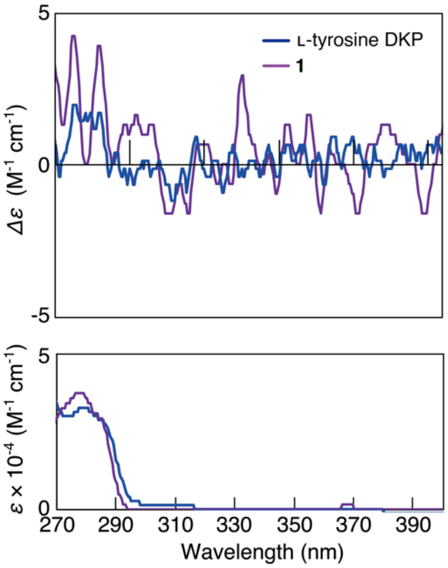

Fig. S12 CD and UV−vis absorption spectra of L-tyrosine DKP and **1** measured in DMF (c = 0.04 mM).

References

S1 A. Sumita, H. Kurouchi, Y. Otani and T. Ohwada, *Chem. Asian J.*, 2014, **9**, 2995–3004.

S2 I. D. Inaloo, S. Majnooni, *Eur. J. Org. Chem.*, 2019, 6359–6368.

S3 M. J. Frisch, G. W. Trucks, H. B. Schlegel, G. E. Scuseria, M. A. Robb, J. R. Cheeseman, G. Scalmani, V. Barone, G. A. Petersson, H. Nakatsuji, X. Li, M. Caricato, A. V. Marenich, J. Bloino, B. G. Janesko, R. Gomperts, B. Mennucci, H. P. Hratchian, J. V. Ortiz, A. F. Izmaylov, J. L. Sonnenberg, D. Williams-Young, F. Ding, F. Lipparini, F. Egidi, J. Goings, B. Peng, A. Petrone, T. Henderson, D. Ranasinghe, V. G. Zakrzewski, J. Gao, N. Rega, G. Zheng, W. Liang, M. Hada, M. Ehara, K. Toyota, R. Fukuda, J. Hasegawa, M. Ishida, T. Nakajima, Y. Honda, O. Kitao, H. Nakai, T. Vreven, K. Throssell, J. A. Montgomery, Jr., J. E. Peralta, F. Ogliaro, M. J. Bearpark, J. J. Heyd, E. N. Brothers, K. N. Kudin, V. N. Staroverov, T. A. Keith, R. Kobayashi, J. Normand, K. Raghavachari, A. P. Rendell, J. C. Burant, S. S. Iyengar, J. Tomasi, M. Cossi, J. M. Millam, M. Klene, C. Adamo, R. Cammi, J. W. Ochterski, R. L. Martin, K. Morokuma, O. Farkas, J. B. Foresman and D. J. Fox, Gaussian 16, Gaussian, Inc., Wallingford CT: 2016.

S4 J. J. P. Stewart, *J. Mol. Model.*, 2013, **19**, 1–32.

S5 S. Grimme, *Chem. Eur. J.*, 2012, **18**, 9955–9964.

S6 S. Grimme, J. Antony, S. Ehrlich and H. Krieg, *J. Chem. Phys.*, 2010, **132**, 154104–154119.

S7 Y. Zhao and D. G. Truhlar, *Acc. Chem. Res.*, 2008, **41**, 157–167.

S8 Y. Zhao and D. G. Truhlar, *Theor. Chem. Acc.*, 2008, **120**, 215–241.

S9 J. Contreras-García, E. R. Johnson, S. Keinan, R. Chaudre, J.-P. Piquemal, D. N. Beratan and W. Yang, *J. Chem. Theory Comput.*, 2011, **7**, 625–632.

S10 J. A. Maier, C. Martinez, K. Kasavajhala, L. Wickstrom, K. E. Hauser and C. Simmerling, *J. Chem. Theor. Comput*., 2015, **11**, 3696－3713.

S11 L. Martinez, R. Andrade, E. G. Birgin and J. M. Martinez, *J. Comput. Chem.*, 2009, **30**, 2157–2164.